Fresenius J Anal Chem (2001) 371 : 106–111
DOI 10.1007/s002160100960

SPECIAL ISSUE PAPER

Ring-Ling Chien · J. Wallace Parce

Multiport flow-control system for lab-on-a-chip microfluidic devices

Received: 20 March 2001 / Revised: 23 May 2001 / Accepted: 31 May 2001 / Published online: 27 July 2001

Abstract A multiport system suitable for pressure control on a lab-on-a-chip microfluidic device is described. An algorithm and a strategy for calculating pressures were developed to control the flow from multiple reservoirs for the microfluidic devices. Dye mixing and enzyme assay titration experiments were performed using pressure-driven flow only. Results show a good linear response over two orders of dynamic range.

Introduction

Microfluidic systems or lab-on-a-chip devices have been extensively studied over the last ten years [1, 2, 3, 4, 5, 6, 7, 8], and proposed for use in capillary electrophoresis (CE), flow injection analysis (FIA), and chemical reaction and synthesis. Microfluidic systems also have been applied to many applications in drug discovery, including high-throughput screening (HTS) for rapid assay of the effects of compounds on various chemical and biochemical systems [9, 10, 11, 12, 13, 14].

One of the advantages of working with microfluidic devices is the ease of fluidic control. The capabilities and implementation of microfluidic systems advanced significantly with the advent of electrokinetics – the use of electrical fields to move fluid materials through the channels of a microfluidic system. Electrokinetic forces have the advantages of direct control, fast response, and simplicity, and enable fluid materials to be selectively moved through a complex network of channels to effect a wide variety of chemical and biochemical analyses. While electrokinetic material transport systems have numerous benefits in the microscale movement, mixing, and aliquoting of fluids, the application of electric fields can have detrimental effects in many instances – for example, the sample-bias effect during sample injection, or perforation or electroporation of the cells in an elevated electric field. In addition, electroosmotic flow depends strongly on the surface property of the devices. The reproducibility and long-term stability of electroosmosis has always been an issue of interest.

To mitigate the problems of electrokinetic systems, hydrodynamic flow is sometimes used in microfluidic systems. The use of external pumps to force liquids directly through microfluidic channels has previously been proposed. Incorporation of mechanical micro pumps and valves within a microfluidic device to move the fluids within a microfluidic channel has also been tested. Unfortunately, the flow rate in the microfluidic systems is usually of the order of nL s^{-1}. Accurate control of such a tiny flow of an incompressible liquid is extremely difficult. Lack of proper control of small pressure differences will yield irreproducible and erratic results. A system that controls the pressure of a compressible gas at the fluid–air interface directly on top of the wells of the microfluidic device is a more practical design. Because the flow impedance of the control line could be made several orders of magnitude smaller than the impedance of the microfluidic channels, the pressure change generated by the control system is transferred completely to the microfluidic device.

In this manuscript, we will describe a system capable of controlling the flow in microfluidic devices using hydrodynamic flow. The basic physics that govern hydrodynamic flow is very similar to that controlling the electrokinetic flow. In microfluidic devices with electrokinetic control one could operate in either voltage control or current control mode. It was generally agreed that the control of the flow in microfluidic devices by means of the electric current is more convenient than the control by voltage and is more relevant to the end user performing chemical and biochemical assays. For hydrodynamic flow, the pressure is equivalent to the voltage and the bulk flow rate is equivalent to the electric current. Similar to electrokinetic control, one would like to control the flow rate instead of applied pressure in hydrodynamic flow. It is, nevertheless, much more complicated to measure and monitor the flow

R.-L. Chien (✉) · J.W. Parce
Caliper Technologies Corp.,
605 Fairchild Drive, Mountain View, CA 94043, USA
e-mail: ring-ling.chien@calipertech.com

rate, especially at the micro-scale level. A computer algorithm has been devised to translate the hydrodynamic flow rates into controllable pressures for each well on the microfluidic devices.

The algorithm is very similar to network analysis in electric circuits. To perform the flow-to-pressure conversion, a network list showing the connection of multi-level hydrodynamic channels was set up for each chip in a database. The channels connected directly to a well form the lowest level in the virtual network. These channels are physically joined at a variety of "pressure nodes" inside the microfluidic chip. Channels connected between nodes or between a node and a well form the second level of the virtual network. Repetition of this process is necessary until all the channels in the chip can be mapped one-to-one to the virtual network.

To determine the pressure drop of each channel, knowledge of flow rate and the hydrodynamic resistance of that channel is needed. The flow rates from the eight wells in the lowest levels of the virtual network are specified by the user. Because the connection is known, the flow rate of any channel in the network could then be obtained by propagating through the network, in accordance with Kirchhoff's current law, which states that the algebraic sum of the currents entering any node is zero. The flow resistances of the channels in a microfluidic chip could be calculated on the basis of chip design and reagent viscosity. When the hydrodynamic resistances and the flow rates are known, the pressure drop in any channel in the network could be calculated using Ohm's law. The external pressure supplied to each well is then obtained by summing all the pressure drops along the virtual network starting from the node at the top level.

Assuming the hydrodynamic resistance is known, this multiport pressure system provides highly precise flow control from each individual channel within a microfluidic network. This capability is well suited for many applications such as reagent dilution, enzyme assays, and chemical reactions.

Experimental

Multiport control system. Figure 1 shows a schematic diagram of our system capable of providing multiple pressure or voltage/current control coupled with a multi-reservoir microfluidic device to manipulate the movement of fluids within microfluidic channel networks. A home-made eight-syringe pump system is used as our pressure or vacuum source. The syringe pump is driven by plungers made by either Kloehn (Model 50120, Las Vegas, NV, USA) or Cavaro Scientific Instruments (Model XP3000, Sunnyvale, CA, USA). The plunger drive has a travel distance of approximately 30 mm and a micro-stepper with resolution of 24,000 steps. The speed of the plunger can be varied in real time from 1.2 s to 20 min per full stroke. Each syringe in the system can be addressed and operated individually by a PC through a RS232/RS485 serial connection.

Since the speed of plunger is very fast, the response time of the syringe pump is mostly limited by the dead volume and the syringe size. Although one could easily build an extremely fast pump by using a large-volume syringe, large-volume syringes will yield less resolution in pressure control. To achieve a compromise between speed and sensitivity, we used 10-mL syringes as our standard size. In some special circumstances when higher resolution was desired we used 1 mL or 500 μL syringes.

The other advantage of a syringe pump system is high accuracy and absence of pulsation noise. The sensitivity of our system is generally limited by the pressure sensor and A/D noise. If the system is leak-tight, we easily achieve the resolution of 0.001 psig for a 5 psig sensor. (1 psig=6894.76 Pa) As alternatives to the syringe pump, a peristaltic pump or other pressure sources could also be used.

The output of each syringe is then connected to a three-port valve with a 250 ms turn time between adjacent ports. The valve is driven by a stepper motor with optical encoder for position feedback. One port is open to ambient to enable the syringe pump to release or calibrate the pressure. The other port is attached directly to another three-way Tee that is connected to a sensor that monitors the pressure of the pump. For a microfluidic device controlled by hydrodynamic means one generally prefers to operate at low pressure to simplify chip design and obtain a reasonable flow rate and

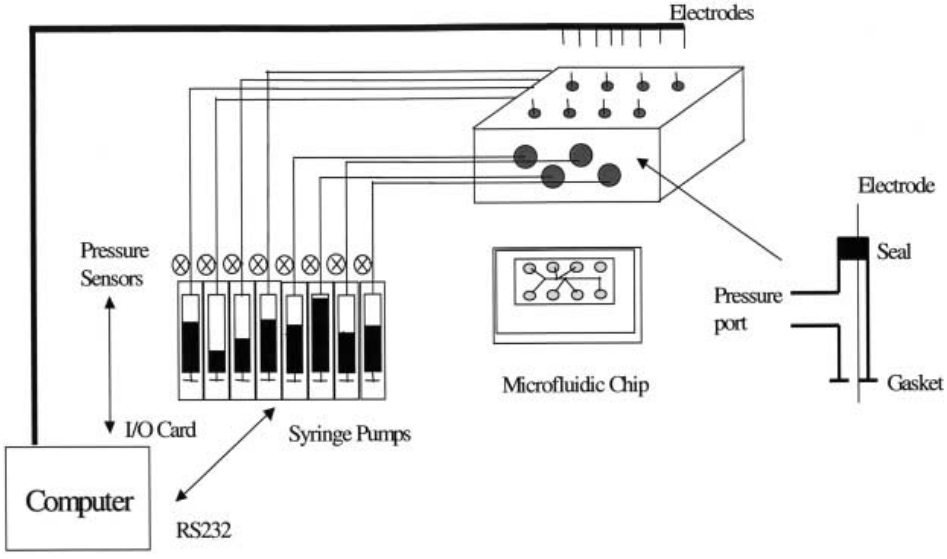

Fig. 1 A schematic diagram of the universal multiport system. One of the eight Tee sections in the chip interface is also shown in the expanded view

reaction time. One would, on the other hand, like to operate at a pressure much higher than the hydrostatic and capillary pressure exerted by the buffer in the wells, to avoid pressure noise. This capillary pressure is generally in the order of one hundredth psig, so a sensor with a maximum pressure of approximately 1 to 5 psig will yield a reasonable dynamic range. For most applications, we used miniature pressure sensors (Model PX185 or 186) from Omega Engineering (Stamford, CT, USA). These sensors are relatively inexpensive and have a repeatability of ±0.15% FS. They have a fully amplified and conditioned output in the range 1–6 V dc. The output is connected to a CB-50 connector block and DAQ-Card-1200 or PCI1200 devices (National Instruments, Austin, TX, USA). The control program and the user interface are written in LabView (National Instruments, Austin, TX, USA).

The other end of the sensor Tee is connected to PEEK or Teflon tubing connected to a pressure manifold to interface with the microfluidic device. Because the sensor is located far from the microfluidic devices, the pressure-transmission system must have relatively low impedance so that the pressure change generated by the syringe pump will be transferred accurately and completely to the device. Because the channel depth of the devices used is generally of the order of 10 μm, 100-μm i.d. tubing was used. To a first-order approximation the hydrodynamic impedance is inversely proportional to the fourth power of radius. Consequently, the impedance in the pressure transmission lines is at least several orders of magnitude smaller than the impedance of the channel on microfluidic devices. In addition, ambient air as the compressible medium was used, which makes the control even faster and more reliable.

At the end of the pressure transmission system, the tubing is coupled to a manifold for chip interface. Several different designs of chip interface manifold were tested. Figure 1 shows a universal manifold suitable for either electrokinetic or hydrodynamic control or a combination of both. This manuscript will report the results obtained from hydrodynamic control only.

In this universal chip manifold, eight T-channels were made on the block to interface with the reservoirs on a microfluidic device. A piece of rubber gasket with eight holes was glued to the bottom of the block to make vacuum seal as the manifold was screwed down on to the mounting plate. Platinum electrodes were inserted in one end of T-channels and epoxy glue was used to fix the electrodes and ensure a vacuum seal. The other end of the T-channel has 1/4–28 fitting and is connected to the syringe pump for pressure control.

For each system, the syringe drive was calibrated in advance by pulling a fixed number of steps. The change of pressure is measured and stored in the program as calibration data. The real-time control of any pressure change is then achieved very rapidly based on the gas law, PV=nRT, and the calibration data. The response time of the system obviously depends on many factors, for example dead volume, syringe size, etc. For or system the response time is less than 500 ms for a pressure change from 0 to 1 psig.

Chip design and fabrication. To utilize the full range of controllability of the pump, the chip design must be optimized for hydrodynamic flow. One problem in flow control in microfluidic devices is the noise from secondary hydrostatic forces such as capillary forces within reservoirs. To reduce these unwanted effects the flow resistance from each well must be large enough such that a maximum variation of flow rate can be achieved within the dynamic range of operating pressure. This can be achieved by using a shallow channel or flow restrictors. Alternatively, one could also enhance channel resistance by using a long serpentine path. One example of a chip designed for pressure flow is shown in Fig. 2. The side channels have a resistance of the order of 1.3×10^{11} g cm^{-4} s. The main channel has a resistance of 4.8×10^{10} g cm^{-4} s. For a pressure drop between reservoirs of approximately 2 psig, this chip will provide a mixing time of approximately 6 s and a reaction time of approximately 20 s. The chip is designed to have roughly 1/3 flow from each pair-well. If 100% flow is from any branch, the pressure drop across that branch will be beyond the dynamic range of the system.

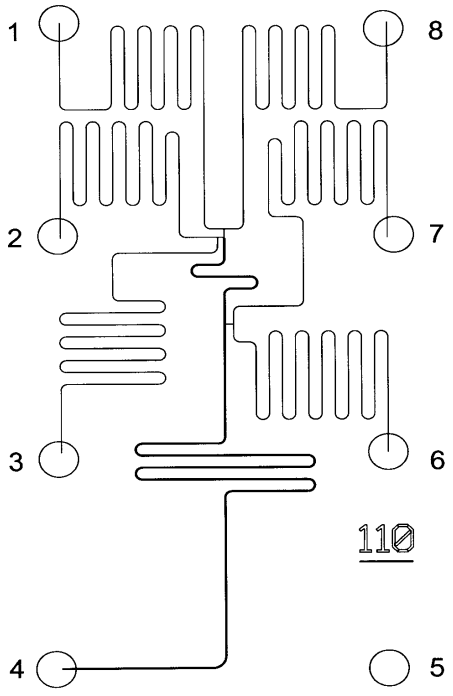

Fig. 2 Chip design optimized for hydrodynamic flow control. The chip has the pair-well design suitable for dilution and enzymatic studies

Another feature of the chip shown in Fig. 2 is the so called pair-well design. If the chip is filled with buffers of the same viscosity, the pressure on all junctions can be predicted in advance from a knowledge of the geometry and the flow rate of the main channel. Because the two channels for the pair-well are connected to the common node, and have same hydrodynamic resistances, the change of flow in one channel could be easily compensated by that from another channel by varying the same amount of pressure in opposite direction without changing the flow in the main channel. By varying the relative pressure of a two pair-well connected to the common node, highly reproducible and rapidly changeable concentrations can be created to determine standard curves for a chemical reaction.

A standard semiconductor photolithography process is used to wet-etch channels, as reported previously [11, 12, 13, 14, 15]. Two different channel widths, 5 μm and 50 μm were used on the mask; this resulted, after etching, in channels 29 μm deep and 74 μm wide. The chips were made from two layers of soda lime glass. The top layer contained an array of eight 2-mm diameter holes. Reagent wells were created by sandwiching the etched layer with the top layer of glass, and bonded together by a high-temperature thermal process. After bonding, the chips were thoroughly cleaned with deionized water.

Microscope and detection system. A modified Nikon TE300 inverted microscope with a 50-W tungsten–halogen light source was used for epi-fluorescence detection in this experiment. Two additional threaded holes were added to the microscope stage to mount the chip interface manifold described above. There is no overhead light for transmission microscopy. For examining chips visually, LED lights are provided in the chip interface and controlled by means of a separate 9-V power supply.

A D-104 photometer from PTI Technology was attached to the side port of the Nikon TE300 microscope and used as the detection system. The PMT output is sent directly to a home-made current and voltage controller. All data-collection software was designed in-house and run on a PC.

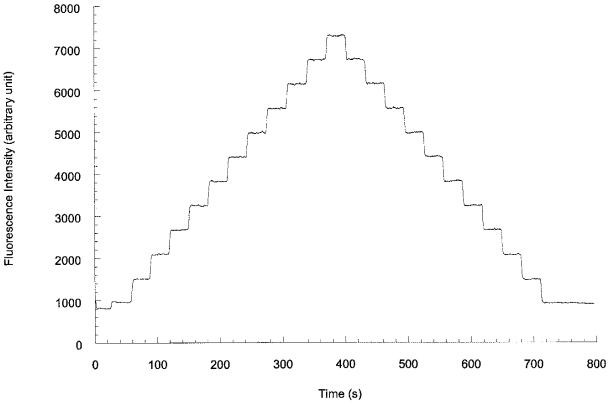

Fig. 3 Fluorescence signal showing series dilution and mixing of a dye and an aqueous solution

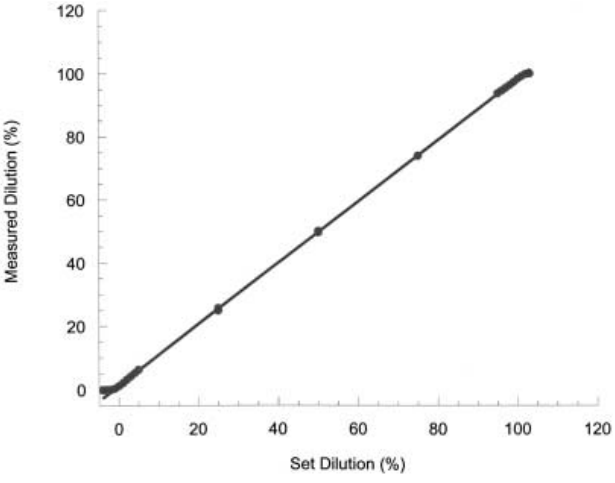

Fig. 4 A plot of measured dilution ratio against set dilution ratio. The measured dilution is normalized with respect to the saturated signal and corrected for background signal

Results and discussion

Pair-well dilution

The first experiment was performed to show the ability to control fluid dilutions precisely. On-chip dilution in microfluidic devices using electrokinetic force only has previously been demonstrated [15]. Similar control using hydrodynamic means should be shown.

The many different combinations which could be used for chip design shown in Fig. 2. To perform a dilution using wells 1 and 8, a script of pressure settings was generated automatically to set the relative flow of dye from well 1 from –4% to +44%, with 10% step size, of the total flow. The negative flow means the fluid was directed in opposite direction, flowing back into the reagent well. The flow from well 8 was correspondingly changed from +44% to –4% of the total flow, to represent 0 to 100% mixing between pair-wells 1 and 8.

In the experiment, 1 μmol L^{-1} fluorescein dye was placed in wells 1 and 3. Water was used in all other wells. The flow from wells 2, 3, 6, and 7 was set to a constant 15% each. The remaining 40% flow comes from wells 1 and 8. Because the flow from well 3 is kept constant, the extra dye signal introduces a constant offset. Figure 3 shows the raw dye fluorescence data as measured by a PMT downstream of the intersection node. The step was very clean and controllability was excellent.

By continuous increasing of the pressure on the dye well, the fluorescence signal will eventually be saturated and stabilized when the main channel is filled with 100% fluorescein dye from dye wells. Knowing this saturated level and the blank baseline background, the calibrated measured dilution can be plotted against set dilution as shown in Fig. 4. The results are indicative of very good agreement between predicted and observed values. The

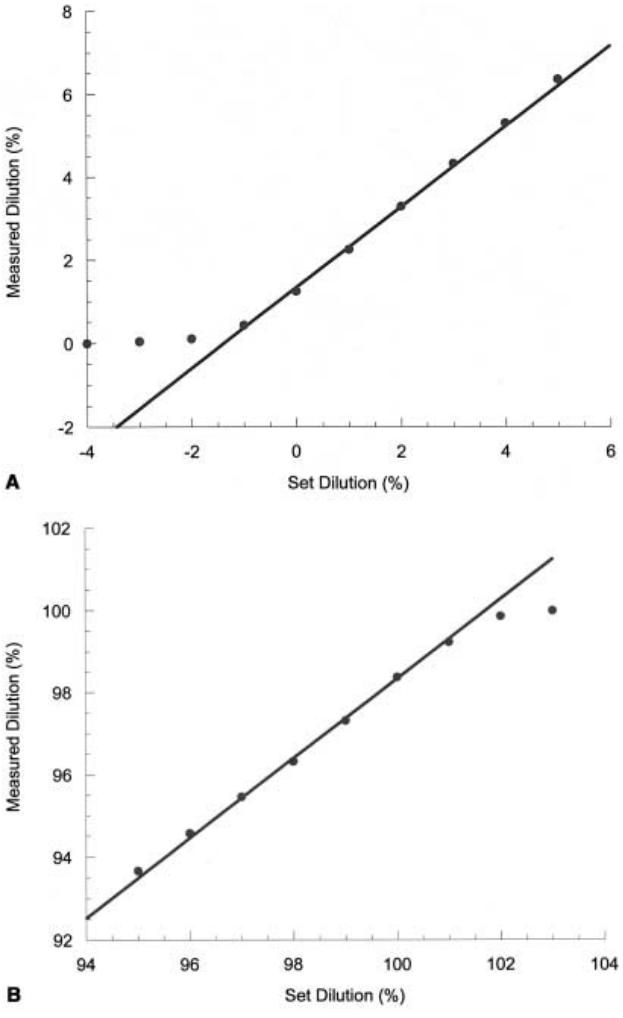

Fig. 5 (**a**) Same as Fig. 4 but the range is set at the low end between –4 and 6%. (**b**) Same as (**a**) but the range is set at the high end between 94 and 104%. The plots show a good linear relationship over two orders of dynamic range. A slight offset is observed between set and measured dilution

small offset of zero flow or 100% flow, as shown in Fig. 5 (a) and (b), respectively, indicates the channel geometry can be slightly different from the simulation. This discrepancy could be reduced further if the channel geometry was calibrated in advance by measuring the electrical resistance of a conducting standard in the channel.

Enzyme assay

Characterization of an enzyme usually involves determination of maximum reaction velocity, Vmax, and of a "Michaelis constant", Km, for each substrate. Microchip-based enzyme assays have been demonstrated by many groups [16, 17, 18]. Electroosmosis was usually used to transport these reagents into the network of etched channels, where the enzymatic reaction occurs. Because electroosmosis is very sensitive to the change of surface property, it is sometimes better to perform the assay using pressure flow only.

The chip shown in Fig. 2 is designed to perform enzyme kinetic studies using a pressure-driven system for fluorogenic assays. The enzymatic reaction of alkaline phosphatase on DiFMUP was chosen as an example. Cleavage of the non-fluorogenic peptide substrate by the enzyme provides the fluorescence signal that could be monitored in the flow stream of the main incubation channel. In a typical arrangement, the enzyme is placed in well 7 and the substrate is placed in both wells 1 and 3 to increase the dynamic range. Assay buffer is placed in the remaining wells. The flow is fixed at 40%, 30%, and 30% for pair-wells 1 and 8, 2 and 3, and 6 and 7, respectively. By changing the relative pressures on the pair wells, either enzyme concentration or substrate concentration could be varied in real time on a single chip. The diluted enzyme and substrate then flow into the main channel. The incubation time is controlled by the vacuum applied to the waste well.

A script containing the step, duration, and contribution of flow from each well was used to run the experiment automatically step by step. The raw data from the PMT detector are shown in Fig. 6. In the experiment the fluorescence signal from the substrate only was obtained first by holding the contribution from the enzyme well to zero. The substrate was then titrated for 10 different concentrations from 0 to 70% of total flow. After obtaining the substrate-only signal, the flow from the enzyme well was set to 30% and the same dilution steps were repeated again. The whole experiment required approximately 15 min and the quality and reproducibility of the data are excellent.

In a traditional enzyme kinetic study, the reaction rate for each concentration of substrate is measured as the slope of the signal against time. In theory we could perform similar time-dependent experiments by changing the flow rate in the main reaction channel. It is, however, much simpler to perform a fixed-time experiment with constant flow rate in the main channel. If the reaction time is short enough, which is usually true in a microchip system, the signal will be directly proportional to the initial reaction rate after subtracting the background signal generated from substrate only. A plot of background corrected signal against substrate concentration is shown in Fig. 7.

The data from this substrate titration experiment were evaluated using a double-reciprocal (Lineweaver–Burk) transformation. The resulting plot is shown in Fig. 8. From this plot, the Km is 1.6 mmol L^{-1}.

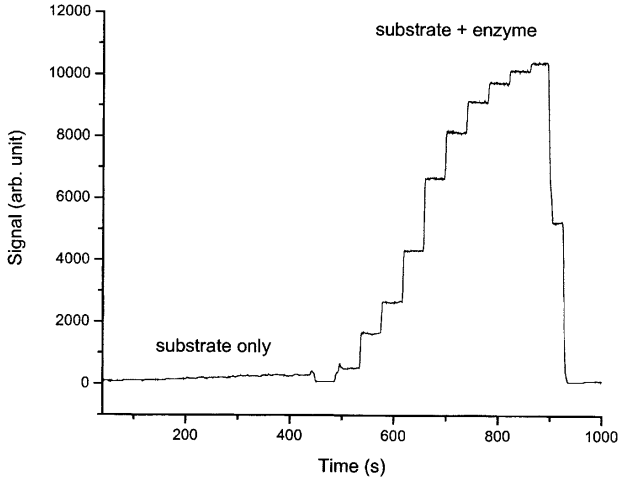

Fig. 6 Raw data showing fluorescence signal from a continuous-flow fluorogenic enzyme titration. The signal from the substrate only was obtained first by holding the contribution from the enzyme well to zero. The substrate was then titrated for 10 different concentrations from 0 to 70% of total flow. After obtaining the substrate-only signal, the flow from the enzyme well was set to 30% and the same dilution steps were repeated

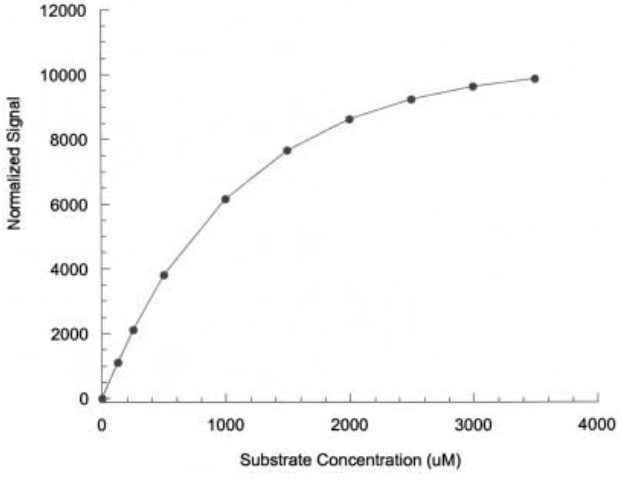

Fig. 7 The plot of reaction rate against substrate concentration for alkaline phosphatase assay using pressure-driven flow. The substrate is DiFMUP

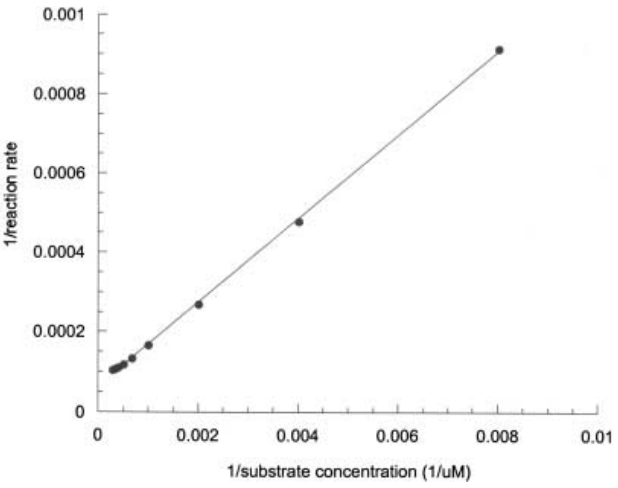

Fig. 8 The Lineweaver–Burk plot for determination of Km using pressure-driven flow

Conclusions

Lab-on-a-chip devices provide a novel format for biochemical experimentation. The ability to program and control fluid transport has always been the most promising feature of lab-on-a-chip devices. The universal multiport system described is capable of controlling multiple pressures on wells in a lab-on-a-chip microfluidic device. In addition to simple dye dilution, other experiments involving more complicated flow control were performed. The ability to perform plug injection using hydrodynamic control only was also demonstrated. Because our system was not optimized for fast response, the plug profile is much broader than the profile obtained from electrokinetic injection. It is, nevertheless, possible to reduce the time constant by using larger syringe pumps with faster speeds. The universal chip interface also has build-in electrodes that enable electrokinetic flow control. Further work is currently in progress on other applications involving combination of hydrodynamic and electrokinetic flows.

Acknowledgments The microchip used in this work was designed by Dr Michael Spaid. The authors also thank Alex Gefter and Michael Kennedy for engineering support, Jill Coffin for performing enzyme assay, and Drs Theo Nikiforov, Anne Kopf-Sill, and Andrea Chow for many helpful discussions and suggestions.

References

1. Manz A (1991) Trends Anal Chem 10:144
2. Manz A, Graber N, Widmer HM (1988) Sens Actuators 14:101
3. Harrison DJ, Manz A, Fan Z, Ludi H, Widmer HM (1992) Anal Chem 64:1926–1932
4. Harrison DJ, Fluri K, Seiler K, Fan Z, Effenhauser CS, Manz A (1993) Science 261:895–897
5. Woolley AT, Matthies RA (1995) Anal Chem 67:3676–3680
6. Jacobson SC, Hergenroder R, Koutny LB, Warmack RJ, Ramsy JM (1994) Anal Chem 66:1107–1113
7. Jacobson SC, Ramsey JM (1997) In Landers JP (ed) Handbook of Capillary Electrophoresis, 2nd edn, John Wiley and Sons, New York, pp 827–839
8. Harrison DJ, van den Berg A (1998) (eds) Micro Total Analysis System '98, Kluwer Academic Publishers, The Netherlands
9. Chiem N, Harrison JD (1997) Anal Chem 69:373–378
10. Koutny LB, Schmalzing D, Taylor TA, Fuchs M (1996) Anal Chem 68:18–22
11. Cohen CB, Chin-Dixon E, Jeong S, Nikiforov T (1999) Anal Biochem 273:89–97
12. Sundberg SA, Chow A, Nikiforov T. Wada HG (2000) Drug Discovery Today: HTS Supplement 1:S42-S53
13. Sundberg SA (2000) Curr Opin Biotechnol 11, 47–53
14. Bousse L, Cohen CB, Nikiforov T, Chow A, Kopf-Sill A, Dubrow R, Parce JW (2000) Annu Rev Biophys Biomol Struct 29:155–81
15. Kopf-Sill A, Nikiforov T, Bousse L, Nagle, R, Dubrow R, Parce JW (1997) SPIE 2978:172–179
16. Hadd AG, Raymond DE, Halliwell JW, Jacobson SC, Ramsey JM (1997) Anal Chem 69:3407–3412
17. Hadd AG, Jacobson SC, Ramsey JM (1999) Anal Chem 71: 5206–5212
18. Li P, Harrison DJ (1997) Anal Chem 69:1564–1568